Armstrong JL, Hill DS, McKee CS, Hernandez-Tiedra S, Lorente M, Lopez-Valero I, Anagnostou ME, Babatunde F, Corazzari M, Redfern CPF, Velasco V, Lovat PE. Exploiting Cannabinoid-Induced Cytotoxic Autophagy to Drive Melanoma Cell Death. *Journal of Investigative Dermatology* 2015, 135(6), 1629-1637.

DOI link to article:

http://dx.doi.org/10.1038/jid.2015.45

Date deposited:

24/06/2015

Embargo release date:

10 August 2015

Exploiting cannabinoid-induced cytotoxic autophagy to drive melanoma cell death

Jane L Armstrong[1,2], David S Hill[1], Christopher S McKee[1], Sonia Hernandez-Tiedra[3], Mar Lorente[3], Israel Lopez-Valero[3,4], Maria Eleni Anagnostou[1], Fiyinfoluwa Babatunde[1], Marco Corazzari[5], Christopher PF Redfern[6], Guillermo Velasco[3,4*], Penny E Lovat[1*]

[1]Dermatological Sciences, Institute of Cellular Medicine, Newcastle University, Newcastle-upon-Tyne, UK

[2]Faculty of Applied Sciences, University of Sunderland, Sunderland, UK

[3]Department of Biochemistry and Molecular Biology I, School of Biology, Complutense University, Madrid, Spain

[4]Instituto de Investigaciones Sanitarias San Carlos (IdISSC), 28040 Madrid, Spain

[5]Department of Biology, University of Rome 'Tor Vergata', Rome, Italy

[6]Northern Institute for Cancer Research, Newcastle University, Newcastle-upon-Tyne, UK

*GV and PEL are joint senior authors.

Running Title: Cytotoxic autophagy in melanoma

Key words: Cannabinoids, autophagy, apoptosis, melanoma

.

Abbreviations

THC Δ^9-Tetrahydrocannabinol
CBD cannabidiol

Corresponding author: Dr Penny Lovat
Dermatological Sciences
Institute of Cellular Medicine
The Medical School
Newcastle University
Framlington Place
Newcastle upon Tyne
NE2 4HH
e mail: penny.lovat@ncl.ac.uk
Tel: +44 191 2227170
Fax: +44 191 2227179

Word count: 3490
Figures: 6

Abstract

While the global incidence of cutaneous melanoma is increasing, survival rates for patients with metastatic disease remain less than 10%. Novel treatment strategies are therefore urgently required, particularly for patients bearing BRAF/NRAS wildtype tumours. Targeting autophagy is a novel means to promote cancer cell death in chemotherapy-resistant tumours and the aim of the present study was to test the hypothesis that cannabinoids promote autophagy-dependent apoptosis in melanoma. Treatment with Δ^9-Tetrahydrocannabinol (THC) resulted in the activation of autophagy, loss of cell viability and activation of apoptosis, while co-treatment with chloroquine or knockdown of Atg7, but not Beclin-1 or Ambra1, prevented THC-induced autophagy and cell death *in vitro*. Administration of Sativex-like (a laboratory preparation comprising equal amounts of THC and cannabidiol (CBD)) to mice bearing BRAF wildtype melanoma xenografts substantially inhibited melanoma viability, proliferation and tumour growth paralleled by an increase in autophagy and apoptosis compared to standard single agent temozolomide. Collectively our findings suggest THC activates non-canonical autophagy-mediated apoptosis of melanoma cells, suggesting cytotoxic autophagy induction with Sativex warrants clinical evaluation for metastatic disease.

Introduction

Cutaneous melanoma incidence continues to increase, and response rates of patients with metastatic melanoma to current therapy remain poor (Garbe et al., 2011). Identification of driver mutations and development of targeted therapies to BRAF/MEK has revolutionised melanoma therapy, though clinical resistance is inevitable (Chen and Davies, 2014). The emergence of immunotherapies able to promote tumour T-cell responses are further changing melanoma management (Wolchok et al., 2010), however, not all patients respond (Prieto et al., 2012). It is therefore clear there is no consistently beneficial treatment for metastatic melanoma and alternative approaches should be explored.

Autophagy (macroautophagy) is the principal lysosomal-mediated mechanism for the degradation of damaged or long-lived organelles and proteins. Under physiological conditions, autophagy maintains normal turnover of cellular components as well as responding to metabolic stress, while in pathological settings autophagy activation mediates defence against extracellular insults and pathogens (Choi et al., 2013). The current model for the role of autophagy in cancer is that in the early stages of tumour development, quality control by autophagy inhibits tumourigenesis, while in advanced cancer, autophagy provides energy to meet the increased demands and a means to resist cell death caused by cytotoxic therapy (White, 2012). Preclinical data suggest lysosomal inhibition can cause tumour regression, and the lysosome inhibitors chloroquine or hydroxychloroquine are now being evaluated in clinical trials either alone or in combination with chemotherapy (Yang et al., 2011). However, recent studies suggest chloroquine/hydroxychloroquine treatment may promote tumour development (Michaud et al., 2011, Maycotte et al., 2012), questioning the benefit of autophagy inhibition. An alternative approach for autophagy modulation is via exacerbation; while initially this appears counterintuitive to treat advanced cancer, recent evidence suggests that in particular circumstances a consequence of autophagy activation is cell death (Ding et al., 2007, Scarlatti et al., 2008, Tomic et al., 2011, Basit et al., 2013). Therapeutic exploitation of cytotoxic autophagy to drive cancer cell death is therefore an emerging concept for the development of novel cancer treatments.

Cannabinoids are a diverse class of compounds derived from *Cannabis sativa*, with Δ^9-tetrahydrocannabinol (THC) the most relevant owing to its high potency and abundance (Pertwee, 2008). THC exerts its biological effects by mimicking endocannabinoids, which bind to and activate two G protein-coupled cannabinoid receptors, CB1 and CB2 (Howlett et al., 2002). CB1/CB2 receptors are expressed in many cancer cell types (Velasco et al., 2012), and cannabinoids are currently being investigated as anti-cancer agents, including glioblastoma for which THC has shown considerable promise (Velasco et al., 2012). Preclinical data demonstrate THC exerts its anti-tumoural action via induction of endoplasmic reticulum (ER) stress, up-regulation of the transcriptional coactivator p8 and the pseudo-kinase tribbles homologue 3 (TRIB3), the stimulation of autophagy and execution of apoptosis (Carracedo et al., 2006, Salazar et al., 2009a, Salazar et al., 2009b). Blockade of autophagy prevents THC-induced apoptosis and cell death, indicating autophagy is upstream of apoptosis and demonstrating the potential of p8/TRIB3-mediated autophagy as a cytotoxic pathway.

Alongside genetic changes, adaption to ER stress and the aberrant control of autophagy have emerged as key drivers of malignancy and therapy resistance in advanced melanoma (Armstrong et al., 2011, Corazzari et al., 2013). The cannabinoid receptors have previously been identified as potential therapeutic targets (Blazquez et al., 2006, Carracedo et al., 2006),

hence targeting ER stress responses combined with cytotoxic autophagy using cannabinoids may represent a valuable therapeutic approach for metastatic melanoma. The aim of this study was to determine whether THC activates cytotoxic autophagy in melanoma cells *in vitro* and *in vivo*. Our data suggest a non-canonical mechanism of autophagy-mediated apoptosis, highlighting the potential to harness autophagy for therapeutic benefit in advanced melanoma.

Results

THC activates autophagy and apoptosis in melanoma cells

Characteristic features of early and late stages of autophagy were assessed using LC3 lipidation (LC3-II) and analysis of autophagic flux using chloroquine and visualization of tandem mRFP-GFP–tagged LC3 (Kimura et al., 2007) respectively. LC3-II induction was observed in three human melanoma cell lines in response to THC, and LC3-II accumulated further in the presence of chloroquine in both BRAF wildtype (CHL-1) and mutated (A375, SK-MEL-28) melanoma cells. Additionally, increased numbers of LC3-positive autophagosomes (yellow puncta) and autolysosomes (red puncta), and total red fluorescence (CHL-1: t_{43}=4.17, $P < 0.001$; A375: t_{42}=3.289, $P = 0.002$) were observed in A375 and CHL-1 cells in response to THC treatment, indicating activation of autophagic flux (Fig. 1).

THC reduced melanoma cell viability in a dose-dependent manner while having little effect on primary melanocytes at doses up to 6 μM THC (Fig. 2a). Co-treatment of melanoma cells with sub-maximal concentrations of THC and the pan-caspase inhibitor ZVAD-fmk significantly increased cell viability compared to treatment with THC alone (CHL-1: t_{22}=3.962, P=0.0007; A375: t_{16}=3.74, P=0.0018; Fig. 2b) suggesting cell death is caspase-dependent. In addition, the cytochrome *c*-labelled structures present in vehicle-treated cells were substantially reduced in THC-treated cells (Fig. 2c), indicating apoptosis activation.

THC-induced apoptosis is dependent on autophagy

In glioma THC activates apoptosis via a mechanism involving TRIB3 and Beclin-1-dependent autophagy (Carracedo et al., 2006, Salazar et al., 2009b). SiRNA-mediated knockdown of TRIB3 significantly prevented loss of cell viability in response to THC in A375 cells (one-way ANOVA; $F_{5,48}$=5.053, P=0.001; THC compared to vehicle treatment in siCtrl cells; Tukey's $P < 0.05$; Supplementary Fig. 1) demonstrating TRIB3 mediates THC-induced cell death. Furthermore, siRNA-mediated knockdown of Atg7 prevented THC-induced accumulation of LC3-II in the presence of chloroquine (one-way ANOVA; $F_{11,24}$=6.878, $P < 0.001$; CQ compared to CQ+THC treated siCtrl cells contrast $P < 0.05$; Fig. 3A,B). THC-induced caspase 3 cleavage was also inhibited by Atg7 knockdown in A375 (Fig. 3a) as well as in CHL-1 and SK-MEL-28 cells (CHL-1: one-way ANOVA; $F_{5,12}$=6.57, P=0.004; THC compared to vehicle-treated siCtrl cells; Tukey's $P < 0.05$; SK-MEl-28: one-way ANOVA; $F_{3,8}$ =4.646, P=0.037; THC compared to vehicle-treated siCtrl cells; Tukey's $P < 0.05$; Supplementary Fig. 2). Additionally, THC treatment resulted in a significant loss of melanoma cell viability only in the absence of chloroquine or Atg7 siRNA (Fig. 3, Supplementary Fig. 2; post hoc tests, Games-Howell or Tukey's $P < 0.01$). In A375 and SK-MEL-28 cells, knockdown of Atg7 alone had no effect on cell viability; however, in CHL-1

cells down-regulation of Atg7 resulted in a significant loss of cell viability (Tukey's $P < 0.001$; Supplementary Fig. 2a) suggesting basal autophagy is required to maintain viability in these cells. Collectively these data demonstrate THC-induced apoptosis of melanoma cells requires TRIB3 and is mediated by Atg7-dependent autophagy.

Beclin-1 promotes autophagy induction and autophagosome formation (Russell et al., 2013); however, Beclin-1-independent autophagy has been reported (Scarlatti et al., 2008, Grishchuk et al., 2011). Unlike in glioma cells, Beclin-1 knockdown did not prevent THC-induced LC3-II accumulation or caspase 3 cleavage (t_4=4.494, P=0.011; Supplementary Fig. 3a) in A375 cells (Fig. 4a), and THC treatment resulted in a significant loss of cell viability under both control and Beclin-1 knockdown conditions (Welch ANOVA; $F_{5,19.63}$ = 94.53, P<0.001; THC treatments compared to vehicle-treated shRNA cells; Games-Howell $P < 0.001$; Fig. 4a-iii). These results suggest autophagy and subsequent apoptosis occur independently of Beclin-1. Furthermore, knockdown of the Beclin-1 interacting protein Ambra1 failed to prevent THC-induced LC3-II induction and caspase 3 cleavage (t_4=6.097, P=0.004; Supplementary Fig. 3b; Fig. 4b). The effect of Ambra1 knockdown alone on A375 viability was variable, however, THC treatment resulted in a significant loss of cell viability under both control (t_{16}=9.44, P<0.001) and Ambra1 knockdown conditions (t_{16} =10.61, P<0.001) (Fig. 4b-iii). Collectively, these data suggest THC activates non-canonical autophagy-mediated apoptosis of melanoma cells which is dependent on Atg7 but not Beclin-1 or Ambra1.

Cannabinoid treatment stimulates autophagy and apoptosis, and the abrogation of melanoma growth *in vivo*

A 1:1 mixture of sub-maximal doses of THC-botanical drug substance (BDS) and the non-psychoactive cannabinoid CBD-BDS, a laboratory mimic of the clinical cannabinoid Sativex (Sat-L) (an oromucosal spray of standardized cannabis extract comprising equal amounts of THC and CBD (GW Pharmaceuticals)), reduced glioma growth *in vivo* to the same extent as an identical dose of THC (Torres et al., 2011). Treatment of melanoma cells with THC+CBD resulted in a substantial loss of melanoma cell viability at a concentration of 1 μM THC + 1 μM CBD in CHL-1, A375 and SK-MEL-28 cells compared to equivalent concentrations of THC, while temozolomide had little effect (Fig. 5). Temozolomide is an alkylating agent currently indicated as standard single-agent chemotherapy for metastatic melanoma. The *in vivo* relevance of these findings was evaluated in the context of BRAF wildtype melanoma tumours, for which there is a particular demand for novel therapeutic approach in the absence of targeted therapies in this tumour group. CHL-1 xenograft tumours were treated for 20 days with temozolomide, THC or Sativex-like. Both THC and Sativex-like significantly inhibited the growth of xenografts (one-way ANOVA; $F_{3,16}$=9.347, P=0.001; THC or Sat-L compared with vehicle, Sat-L compared to Temozolomide: P<0.05, Fig. 6a). Tumours removed from animals at sacrifice were processed for immunohistochemical analysis of proliferative activity (Ki67), apoptosis (TUNEL) and autophagy (LC3). Ki67 fluorescence differed significantly between drug treatments (Welch ANOVA; $F_{3,16.28}$ =61.363, $P < 0.001$; Fig. 6b), and was significantly reduced in tumours from animals treated with temozolomide, THC or Sativex-like compared to control animals (Games-Howell; $P \leq 0.001$), as well as in tumours from animals treated with THC or Sativex-like compared to those treated with temozolomide (Games-Howell; P<0.001). TUNEL fluorescence also differed significantly between treatments (one-way ANOVA; $F_{3,32}$=13.31, P<0.001), and was higher than control in tumours from animals treated with THC or Sativex-like (Tukey's' $P \leq 0.001$), and higher in tumours from animals treated with Sativex-like compared to those treated with temozolomide

(Tukey's; $P<0.05$) (Fig. 6c). Correspondingly, LC3 fluorescence differed between treatments (one-way ANOVA; $F_{3,32}=3.539$, $P<0.05$), with significantly increased LC3 staining in tumours from animals treated with Sativex-like compared to tumours from animals treated with vehicle or temozolomide (Tukey's: $P\leq0.05$, Fig. 6d). Staining for Ki67, TUNEL and LC3 were not significantly different in tumours from animals treated with THC compared to Sativex-like. Collectively these data suggest THC and Sativex-like are more effective than temozolomide in terms of apoptosis induction and anti-tumour response, further validating the therapeutic relevance of cannabinoid treatment for melanoma.

Discussion

It is apparent that autophagy modulation may offer considerable benefit in cancer treatment; however, potential drawbacks to autophagy inhibition have recently been identified (Michaud et al., 2011, Maycotte et al., 2012, Takahashi et al., 2012, Rosenfeldt et al., 2013). Emerging evidence indicates activation of autophagy can, in some circumstances, promote cell death; stimulation of cytotoxic autophagy therefore represents a novel approach to autophagy modulation (Ding et al., 2007, Scarlatti et al., 2008, Salazar et al., 2009b, Grishchuk et al., 2011, Tomic et al., 2011, Basit et al., 2013). Here, we show that the cannabinoid THC exerts its anti-tumour effect on melanoma cells via activation of non-canonical autophagy and subsequent apoptosis, suggesting cannabinoids may be of clinical benefit for metastatic melanoma.

The molecular mechanisms connecting autophagy to cell death remain poorly understood (Shen and Codogno, 2011), however, reports describing autophagy-dependent apoptosis (Ding et al., 2007, Salazar et al., 2009b, Grishchuk et al., 2011, Tomic et al., 2011) suggest multiple interactions between autophagic and apoptotic machinery. THC exerts its effect via the *de novo* synthesis of the sphingolipid ceramide, leading to the activation of ER stress, TRIB3-dependent inhibition of Akt/mTORC1 signalling and autophagy-mediated apoptosis (Carracedo et al., 2006, Salazar et al., 2009b). TRIB3 has been identified as a key switch between cell survival and apoptosis during stress responses (Shimizu et al., 2012), and the participation of TRIB3 in the melanoma response to THC may direct cellular fate towards apoptosis in the context of ER stress-induced autophagy (Salazar et al., 2013).

Autophagy inhibition using both molecular and pharmacological approaches prevented THC-induced autophagy and apoptosis of melanoma cells. However, THC-induced autophagy was not prevented by knockdown of Beclin-1, suggesting in contrast to glioma, non-canonical autophagy mediates apoptosis in response to THC in melanoma. Beclin-1-independent autophagy may promote caspase-independent cell death (Scarlatti et al., 2008, Basit et al., 2013) as well as apoptosis (Grishchuk et al., 2011, Tomic et al., 2011) suggesting autophagy mechanisms not involving Beclin-1 exist which interact with cell death machinery. Interestingly, in contrast to previous studies (Salazar et al., 2009b), THC-induced autophagy was also independent of Ambra1 in melanoma cells. Ambra1 is a Beclin-1 interacting protein which promotes autophagy by stabilising Beclin-1 complexes (Fimia et al., 2007); while supporting the concept of Beclin-1-independent autophagy activation in response to THC, these data highlight the complex regulation of autophagy which likely occurs in a cell type- and context-specific manner.

Tumour-selective killing can be achieved by targeting pathways which are differentially regulated in cancer cells compared to normal cells. In this respect, we have shown that normal human melanocytes are resistant to THC at concentrations which cause cell death in melanoma cells. This is consistent with studies showing cancerous cells are more sensitive to THC and other cannabinoid receptor ligands than their non-transformed counterparts, despite the presence of functional CB receptors (Velasco et al., 2012). Together with previous studies demonstrating an effect of synthetic ligands of cannabinoid receptors in melanoma (Blazquez et al., 2006), these data support clinical evaluation of cannabinoids in advanced stage disease. Furthermore, THC activates autophagy and apoptosis in both BRAF wildtype and mutated melanoma cell lines, suggesting that despite autophagy deregulation (Corazzari et al., 2013, Armstrong et al., 2011), THC is likely effective in melanoma tumours regardless of BRAF mutation status. Furthermore, our findings show that THC is able to reduce melanoma cell viability and tumour xenograft growth alone, but when lower doses of THC are combined with CBD the anti-tumour effect was enhanced *in vitro* and at least equally effective as the higher dose of single-agent THC *in vivo*. Moreover, CBD induces apoptosis via the production of reactive oxygen species and caspase activation in cancer cells (Massi et al., 2006, Shrivastava et al., 2011), indicating THC and CBD engage different molecular machinery which cooperate to promote tumour cell death (Shrivastava et al., 2011, Torres et al., 2011).

In summary, these data highlight the potential for cannabinoid-induced cytotoxic autophagy as an effective strategy to drive melanoma cell death, supporting the clinical evaluation of Sativex for the treatment of metastatic disease.

Materials and Methods

Cell culture, viability assays, and drug treatment

Melanoma cell lines CHL-1, A375, and SK-MEL-28 were obtained from the American Type Culture Collection in 2006 and cultured as described previously (Armstrong et al., 2007). Cell lines were verified by melan A staining (Flockhart et al., 2009) with *B-RAF/NRAS* mutational status confirmed using Custom TaqMan SNP genotyping assays (Hiscutt et al., 2010) (Applera Europe BV) (last tested February 2014). Prior to drug treatment, culture medium was changed to 0.5% FBS medium. Temozolomide (OSI Pharmaceuticals), and ZVAD-fmk (benzyloxycarbonyl-V-A-D(OMe)-fluoromethylketone) (Tocris Bioscience, Bristol, UK) were added in DMSO, and chloroquine (Sigma) was added in water. For *in vitro* experiments, pure Δ^9-tetrahydrocannabinol (THC) (THC Pharm, Frankfurt, Germany), and CBD (synthesised by Professor Mechoulam and kindly provided by Dr Fernandez Ruiz) were prepared in DMSO. Control incubations contained the same amount of DMSO (0.1-0.2% v/v). For treatment with THC+CBD, pure THC and pure CBD were mixed 1:1 (w/w). Analysis of cell viability was performed using 3-(4,5-dimethylthiazol-2-yl)-2,5-diphenyltetrazolium bromide (MTT; Sigma). For *in vivo* experiments, THC-botanical drug substance (THC-BDS; THC content 67.6% w/w; cannabidiol (CBD) content 0.3% w/w; other individual plant cannabinoids <1.5% w/w), and CBD-botanical drug substance (CBD-BDS; CBD content 65.4% w/w; THC content 2.5% w/w; other individual plant cannabinoids <1.7% w/w) were provided by GW Pharmaceuticals. THC-BDS, and CBD-BDS were

provided as a resin, dissolved in ethanol (100 mg/mL), dried and prepared in DMSO. A 1:1 (w/w) preparation of THC-BDS and CBD-BDS was used to mimic Sativex (Sativex-like; Sat-L). For oral administration THC or Sat-L was solved in 100 µl of sesame oil.

Western blotting and RT PCR analysis

Preparation of whole-cell lysates and Western blotting for LC3B, cleaved caspase 3 (Cell Signalling Technology), Atg7 (Santa Cruz Biotechnology), Beclin-1 (BD Biosciences), and Ambra1 (Novus Biologicals) all diluted 1:4000, and β-actin (Sigma) diluted 1:30000, were performed as described previously (Armstrong et al., 2007). Total RNA was isolated from cells using the RNeasy Mini Kit with DNase digestion (Qiagen) according to the manufacturer's protocol. Reverse transcription (RT)-PCR was performed using the Access RT-PCR system (Promega) using primers for TRIB3 (Carracedo et al., 2006) or ß-actin (Armstrong et al., 2005). PCR products were analysed by electrophoresis on ethidium bromide-stained 2% agarose gels and DNA visualised by exposure to UV light.

siRNA transfections

siRNA for Atg7 (HSS116182), TRIB3 (sc-44426, Santa Cruz Biotechnology) or a non-targeting siRNA (Negative control Low GC Stealth RNAi) (Stealth RNAi, Life Technologies) were transfected into cells in OPTIMEM containing siRNA (2-4 nM) using Lipofectamine RNAiMAX (Life Technologies) according to the manufacturer's specification for reverse transfection. After 24 hours medium was replaced with DMEM containing 0.5% FBS and cells treated with drugs as appropriate.

Retroviral or lentiviral infection

Retroviral expression of mRFP-GFP-LC3 (provided by T. Yoshimori, Osaka University, Japan) (Kabeya et al., 2000, Kimura et al., 2007) was performed as described previously (Armstrong et al., 2011). Lentiviral expression of shAmbra1 or a non-targeting sequence shCtrl (MISSION shRNA, Sigma) was performed by cotransfection of 7.5 µg lentivirus vector (pLKO.1-puro) with 2.5 µg of an expression plasmid for the vesicular stomatitis virus G protein into 293 cells using the calcium precipitation method. After 48 hours, melanoma cells were incubated with virus-containing supernatant supplemented with polybrene (4 µg/mL) for 6–8 hours, and selected for puromycin resistance. Lentiviral expression of shBeclin-1 (V3LHS_349509, Dharmacon) or a non-targeting sequence shCtrl (RHS4346, Dharmacon) was performed by cotransfection of 20 µg lentivirus vector with 5 µg of an expression plasmid for the viral envelope (pMD2.G) and 15 µg packaging plasmid (pCMVdelta8.91) into HEK293T cells using the calcium precipitation method. After 72 hours, melanoma cells were spin-transduced (1.5 hours, 1200 RPM, Harrier 15/80) with virus-containing supernatant supplemented with polybrene (4 µg/mL) and selected for puromycin resistance.

Confocal microscopy

Cells were grown on glass coverslips before fixation in 4% paraformaldehyde. For immunolabelling, cells were incubated with 0.2% Triton X-100 prior to incubation with anti-cytochrome c (BD Biosciences) at room temperature for 1 hour (McGill et al., 2005). Secondary labelling was performed with Oregon Green 488 conjugated to anti-rabbit IgG (Life Technologies). Nuclei were counterstained with TO-PRO-3 iodide (Invitrogen). Cells were imaged under a Leica TCS SP II laser-scanning confocal microscope with LCS Lite 2.61 software (Leica Microsystems), using a 63 x oil objective.

Xenograft mouse model and immunohistochemical analysis

Athymic nude (nu/nu) 5-week-old male mice (Harlan Iberica Laboratory, Spain) were inoculated by subcutaneous injection of 7.5×10^6 CHL-1 cells in 100 μL PBS containing 0.1% glucose. On establishment of tumours 250 mm^3 in volume, mice were randomized into four treatment groups (5–8 mice per group) and treated by daily administration for 20 days with Temozolomide (TMZ; 5 mg/kg, local - peritumoural injection), THC (15/mg/kg, oral gavage), or Sativex (7.5 mg/kg THC-BDS + 7.5 mg/kg cannabidiol (CBD)-BDS, oral gavage). The control group was treated with 100 μL of vehicle (sesame oil). Caliper measurements of tumour length (l) and width (w) were taken each day, and tumour volume calculated as $(4\pi/3) \times (w/2)^2 \times (l/2)$. Mice were humanely killed on the final day of treatment, and tumours extracted and snap frozen in liquid nitrogen before storage at −80°C. Frozen sections (6 μm) prepared on (3-Aminopropyl)triethoxysilane (Sigma)–coated glass slides were fixed in 4% paraformaldehyde before staining by terminal deoxyribonucleotide transferase–mediated dUTP-X nick-end labeling (TUNEL) or with a Ki67 antibody (ab-15580, Abcam) as previously described (Hill et al., 2009). For LC3 immunolabelling, frozen sections were fixed in acetone and incubated with anti-LC3B (ab48394, Abcam) for 1 hour at room temperature. Secondary labelling was performed with Oregon Green 488 conjugated to anti-rabbit IgG (Life Technologies). Cells were imaged under a Leica TCS SP II laser-scanning confocal microscope with LCS Lite 2.61 software (Leica Microsystems), using a 63 x oil objective.

Statistical analysis

Images of LC3, Ki67 and TUNEL staining were analysed using Velocity (v4.3.1) (Improvision Ltd). Total fluorescence was obtained by multiplying pixel number to the mean pixel intensity, after appropriate thresholding. TOPRO-3 fluorescence was determined by the number of pixels with fluorescence above the threshold, which was proportional to nuclei number. For each tumour (3 animals per group, 3 randomly selected images each), values were reported as normalised total fluorescence (total fluorescence (LC3/Ki67/TUNEL) / total nuclear fluorescence) and expressed as fold change relative to the mean value obtained from control animals, from two independent staining analyses. mRFP fluorescence was analysed using ImageJ; data are total pixel intensities/cell minus the mean background fluorescence of nuclei. Homogeneity of variances were checked using Levene's test and if variances were equal (normalised data or after log transformation) data were analyzed by drug treatment with the use of Student's T test or using one-way ANOVA with planned contrasts (LC3

expression) or with Tukey's post hoc test for multiple pair-wise comparisons. Where variances were not equal, Welch ANOVA test was used with Games-Howell post hoc tests for pair-wise comparisons (SPSS Statistics 20 (SPSS Inc.)).

Conflict of Interest

The authors state no conflict of interest

Acknowledgements

The authors thank the Bio-Imaging Unit, Institute of cellular Medicine, Newcastle University, for their assistance with confocal microscopy studies, the late Mr Andrew Walker from the JGW Patterson Foundation for project advice and support, as well as Emma Woodward (Newcastle University) for preparation of Beclin-1 virus particles.

In the UK, this work was supported by the JGW Patterson Foundation, British Skin Foundation, the Newcastle Healthcare Charity, the North Eastern Skin Research Fund, and the Health Sciences and Wellbeing Beacon (University of Sunderland). Work at G Velasco's group was supported by grants from the Spanish Ministry of Economy and Competitiveness/Instituto de Salud Carlos iii (MINECO/ISCiii), the European Regional Development Fund (ERDF/FEDER): PS09/01401; PI12/02248; Fundación Mutua Madrileña, Fundación TELEMARATÓ and GW Pharmaceutical ltd.), the Comunidad de Madrid and the Spanish Ministry of Education and Science. Work by M Corazzari was supported by the Associazione Italiana per la Ricerca sul Cancro.

References

Armstrong JL, Corazzari M, Martin S, *et al* (2011). Oncogenic B-RAF signaling in melanoma impairs the therapeutic advantage of autophagy inhibition. *Clin Cancer Res* 17:2216-2226.

Armstrong JL, Ruiz M, Boddy AV, *et al* (2005). Increasing the intracellular availability of all-trans retinoic acid in neuroblastoma cells. *Br J Cancer* 92:696-704.

Armstrong JL, Veal GJ, Redfern CP, *et al* (2007). Role of Noxa in p53-independent fenretinide-induced apoptosis of neuroectodermal tumours. *Apoptosis* 12:613-622.

Basit F, Cristofanon S, Fulda S (2013). Obatoclax (GX15-070) triggers necroptosis by promoting the assembly of the necrosome on autophagosomal membranes. *Cell Death Differ* 20:1161-1173.

Blazquez C, Carracedo A, Barrado L, *et al* (2006). Cannabinoid receptors as novel targets for the treatment of melanoma. *FASEB J* 20:2633-2635.

Carracedo A, Lorente M, Egia A, *et al* (2006). The stress-regulated protein p8 mediates cannabinoid-induced apoptosis of tumor cells. *Cancer Cell* 9:301-312.

Chen G, Davies MA (2014). Targeted Therapy Resistance Mechanisms and Therapeutic Implications in Melanoma. *Hematol Oncol Clin North Am* 28:523-536.

Choi AM, Ryter SW, Levine B (2013). Autophagy in human health and disease. N *Engl J Med* 368:651-662.

Corazzari M, Fimia GM, Lovat P, *et al* (2013). Why is autophagy important for melanoma? Molecular mechanisms and therapeutic implications. *Sem Cancer Biol* 23:337-343.

Ding WX, Ni HM, Gao W, *et al* (2007). Differential effects of endoplasmic reticulum stress-induced autophagy on cell survival. *J Biol Chem* 282:4702-4710.

Fimia GM, Stoykova A, Romagnoli A, *et al* (2007). Ambra1 regulates autophagy and development of the nervous system. *Nature* 447:1121-1125.

Flockhart RJ, Armstrong JL, Reynolds NJ, *et al* (2009). NFAT signalling is a novel target of oncogenic BRAF in metastatic melanoma. *Br J Cancer* 101:1448-1455.

Garbe C, Eigentler TK, Keilholz U, *et al* (2011). Systematic review of medical treatment in melanoma: current status and future prospects. *Oncologist* 16:5-24.

Grishchuk Y, Ginet V, Truttmann AC, *et al* (2011). Beclin 1-independent autophagy contributes to apoptosis in cortical neurons. *Autophagy* 7:1115-1131.

Hill DS, Martin S, Armstrong JL, *et al* (2009). Combining the endoplasmic reticulum stress-inducing agents bortezomib and fenretinide as a novel therapeutic strategy for metastatic melanoma. *Clin Cancer Res* 15:1192-1198.

Hiscutt EL, Hill DS, Martin S, *et al* (2010). Targeting X-linked inhibitor of apoptosis protein to increase the efficacy of endoplasmic reticulum stress-induced apoptosis for melanoma therapy. *J Invest Dermatol* 130:2250-2258.

Howlett AC, Barth F, Bonner TI, *et al* (2002). International Union of Pharmacology. XXVII. Classification of cannabinoid receptors. *Pharmacol Rev* 54:161-202.

Kabeya Y, Mizushima N, Ueno T, *et al* (2000). LC3, a mammalian homologue of yeast Apg8p, is localized in autophagosome membranes after processing. *EMBO J* 19:5720-5728.

Kimura S, Noda T, Yoshimori T (2007). Dissection of the autophagosome maturation process by a novel reporter protein, tandem fluorescent-tagged LC3. *Autophagy* 3:452-460.

Massi P, Vaccani A, Bianchessi S, *et al* (2006). The non-psychoactive cannabidiol triggers caspase activation and oxidative stress in human glioma cells. *Cell Mol Life Sci* 63:2057-2066.

Maycotte P, Aryal S, Cummings CT, *et al* (2012). Chloroquine sensitizes breast cancer cells to chemotherapy independent of autophagy. *Autophagy* 8:200-212.

McGill A, Frank A, Emmett N, *et al* (2005). The anti-psoriatic drug anthralin accumulates in keratinocyte mitochondria, dissipates mitochondrial membrane potential, and induces apoptosis through a pathway dependent on respiratory competent mitochondria. *FASEB J* 19:1012-1014.

Michaud M, Martins I, Sukkurwala AQ, *et al* (2011). Autophagy-dependent anticancer immune responses induced by chemotherapeutic agents in mice. *Science* 334:1573-1577.

Pertwee RG (2008). The diverse CB1 and CB2 receptor pharmacology of three plant cannabinoids: delta9-tetrahydrocannabinol, cannabidiol and delta9-tetrahydrocannabivarin. *Br J Pharmacol* 153:199-215.

Prieto PA, Yang JC, Sherry RM, *et al* (2012). CTLA-4 blockade with ipilimumab: long-term follow-up of 177 patients with metastatic melanoma. *Clin Cancer Res* 18:2039-2047.

Rosenfeldt MT, O'Prey J, Morton JP, *et al* (2013). p53 status determines the role of autophagy in pancreatic tumour development. *Nature* 504:296-300.

Russell RC, Tian Y, Yuan H, *et al* (2013). ULK1 induces autophagy by phosphorylating Beclin-1 and activating VPS34 lipid kinase. *Nat Cell Biol* 15:741-750.

Salazar M, Carracedo A, Salanueva IJ, *et al* (2009a). TRB3 links ER stress to autophagy in cannabinoid anti-tumoral action. *Autophagy* 5:1048-1049.

Salazar M, Carracedo A, Salanueva IJ, *et al* (2009b). Cannabinoid action induces autophagy-mediated cell death through stimulation of ER stress in human glioma cells. *J Clin Invest* 119:1359-1372.

Salazar M, Lorente M, Garcia-Taboada E, *et al* (2013). The pseudokinase tribbles homologue-3 plays a crucial role in cannabinoid anticancer action. *Biochim Biophys Acta* 1831:1573-1578.

Scarlatti F, Maffei R, Beau I, *et al* (2008). Role of non-canonical Beclin 1-independent autophagy in cell death induced by resveratrol in human breast cancer cells. *Cell Deth Differ* 15:1318-1329.

Shen HM, Codogno P (2011). Autophagic cell death: Loch Ness monster or endangered species? *Autophagy* 7:457-465.

Shimizu K, Takahama S, Endo Y, *et al* (2012). Stress-inducible caspase substrate TRB3 promotes nuclear translocation of procaspase-3. *PloS One* 7:e42721.

Shrivastava A, Kuzontkoski PM, Groopman JE, et al (2011). Cannabidiol induces programmed cell death in breast cancer cells by coordinating the cross-talk between apoptosis and autophagy. *Mol Cancer Ther* 10:1161-1172.

Takahashi A, Kimura T, Takabatake Y, *et al* (2012). Autophagy guards against cisplatin-induced acute kidney injury. *Am J Pathol* 180:517-525.

Tomic T, Botton T, Cerezo M, *et al* (2011). Metformin inhibits melanoma development through autophagy and apoptosis mechanisms. *Cell Death Dis* 2:e199.

Torres S, Lorente M, Rodriguez-Fornes F, *et al* (2011). A combined preclinical therapy of cannabinoids and temozolomide against glioma. *Mol Cancer Ther* 10:90-103.

Velasco G, Sanchez C, Guzman M (2012). Towards the use of cannabinoids as antitumour agents. *Nat Rev Cancer* 12:436-444.

White E (2012). Deconvoluting the context-dependent role for autophagy in cancer. *Nat Rev Cancer* 12:401-410.

Wolchok JD, Neyns B, Linette G, *et al* (2010). Ipilimumab monotherapy in patients with pretreated advanced melanoma: a randomised, double-blind, multicentre, phase 2, dose-ranging study. *Lancet Oncol* 11:155-164.

Yang ZJ, Chee CE, Huang S, *et al* (2011). The role of autophagy in cancer: therapeutic implications. *Mol Cancer Ther* 10:1533-1541.

Figure Legends

Figure 1. THC induces autophagy in melanoma cells.
a,b,c, A375, SK-MEL-28 and CHL-1 cells were treated with vehicle or THC (4.5 or 5 μM) for 24 hours, in the presence or absence of chloroquine (CQ; 10 μM) for the final 2 hours, and LC3 and β-actin expression determined by Western blotting. LC3-II expression was quantified and band intensity normalized to β-actin. Data are expressed as fold change relative to the mean LC3-II/β-actin value for a representative experiment and are shown above the western blot (representative data from $n = 3$ independent experiments). D, E, mRFP-GFP-LC3 expressing A375 (d) or CHL-1 (e) cells were treated with vehicle or THC (4.5 μM) for 18 hours. Data are representative fluorescent micrographs (bar, 20 μm) of three independent experiments. f, total red fluorescence values were generated from ≥ 20 cells per treatment condition, from two independent experiments. Pixel intensities were divided by a factor of 10^6 , and data are shown as mean ± SD (** $P < 0.01$, *** $P < 0.001$ *versus* control for each cell line).

Figure 2. THC induces apoptosis of melanoma cells.
a, primary melanocytes, A375, and CHL-1 cells were treated with vehicle or THC (3-10 μM) for 24 hours. b, A375 (i) or CHL-1 (ii) cells were treated with vehicle or THC (5 μM) in the presence or absence of ZVAD (20 μM) for 24 hours. Cell viability was determined by MTT assay. Data generated in triplicate were expressed relative to the mean of vehicle-treated cells in each experiment, for three independent experiments, and shown as mean ± SD (T-test; ** $P < 0.01$, *** $P < 0.001$ *versus* THC+ZVAD). C, A375 cells were treated with THC (5 μM) for 24 hour. Data are representative fluorescent micrographs of cytochrome *c* immunostaining (bar, 20 μm) of three independent experiments.

Figure 3. THC-induced apoptosis requires autophagy
a,b,c, A375 cells were transfected with siRNAs for Atg7 (siAtg7) or with a nonsilencing control siRNA (siCtrl) before treatment with vehicle or THC (4.5, 5 μM) for 24 hours, in the presence or absence of chloroquine (CQ; 10 μM) for the final 2 hours (a,b) or for 24 hours (c). a,b, Atg7, LC3, cleaved caspase 3 and β-actin expression were determined by Western blotting. LC3-II expression was quantified and band intensity normalized to β-actin. Data are expressed as fold change relative to the mean LC3-II/β-actin value for each experiment, for three separate experiments (mean ± SD, $n = 3$). c, Cell viability was determined by MTT assay. Data generated in triplicate were expressed relative to the mean of vehicle-treated siCtrl cells in each experiment, for three independent experiments, and shown as mean ± SD (* $P < 0.05$, ** $P < 0.01$, *** $P < 0.001$ *versus* vehicle treated siCtrl cells).

Figure 4. THC-induced autophagy and cell death is not dependent on Beclin-1 or Ambra1
a, A375 cells stably expressing shRNA for Beclin-1 (shBeclin1) or a nonsilencing control shRNA (shCtrl) were treated with vehicle or THC (4.5, 5 μM) for 48 hours, in the presence or absence presence of chloroquine (CQ; 10 μM) for the final 2 hours (i). Beclin-1, LC3, cleaved caspase 3 and β-actin expression were determined by Western blotting (i). Cell viability (ii) was determined by MTT assay. Data generated in triplicate were expressed relative to the mean of vehicle-treated shCtrl cells in each experiment, for three independent experiments, and shown as mean ± SD (*** $P < 0.001$ *versus* vehicle treated shCtrl cells). b, A375 cells stably expressing shRNA for Ambra1 (shAmbra1) or a nonsilencing control shRNA (shCtrl) were treated with vehicle or THC (5 μM) for 24 hours, in the presence or

absence of chloroquine (CQ; 10 μM) for the final 2 hours (i). Ambra1, LC3, cleaved caspase 3 and β-actin expression were determined by Western blotting (i). Cell viability (ii) was determined by MTT assay. Data generated in triplicate were normalised to the mean of vehicle-treated cells for each shRNA in each experiment, for three independent experiments, and shown as mean ± SD (*** $P < 0.001$ *versus* vehicle treated cells for each shRNA).

Figure 5. Cannabinoids inhibit melanoma cell viability *in vitro*
a,b,c, CHL-1 (a), A375 (b) or SK-MEL-28 (c) cells were treated with Temozolomide (Temo; 10-50 μM), THC (1-5 μM) or THC+CBD (0.5 μM THC + 0.5 μM CBD to 2.5 μM THC + 2.5 μM CBD) for 48 hours. Cell viability was determined by MTT assay. Data generated in triplicate were expressed relative to the mean of vehicle-treated cells for each drug treatment in each experiment, for three independent experiments, shown are mean ± SD for a representative experiment.

Figure 6. THC and Sativex-like cannabinoids promote autophagy and anti-tumour responses in melanoma xenografts
Athymic nude mice were injected subcutaneously in the right flank with CHL-1 melanoma cells. When tumours reached a 250 mm^3 size, mice were treated daily for 20 days with vehicle, Temozolomide (TMZ; 5 mg/kg; local administration), THC (15/mg/kg; oral administration), or Sativex-like (Sat-L; 7.5 mg/kg THC-BDS + 7.5 mg/kg CBD-BDS; oral administration). a, Tumour volumes were measured daily. Each point is the mean from ≥ 5 tumours ± SD and is expressed relative to the tumour volume on day 1 of treatment. b,c,d Immunohistochemical analysis of CHL-1 xenograft tumours treated with Temozolomide, THC or Sat-L. Panels B, C and D are micrographs of tumour sections stained for Ki67 (b), TUNEL (c) or LC3 (d). In each, green is staining for Ki67, TUNEL or LC3, and red is the TO-PRO-3 counterstain. The bar graphs below each set of micrographs summarise the data analysis from tumour sections (bar, 20 μm). Total fluorescence values (total fluorescence (LC3/Ki67/TUNEL) / total nuclear fluorescence) were generated in triplicate for 3 tumours in each treatment group. Data are expressed as fold change relative to the mean value obtained from control animals, from two independent staining analyses, and shown as mean ± SD (** $P < 0.01$, *** $P < 0.001$ *versus* control animals).

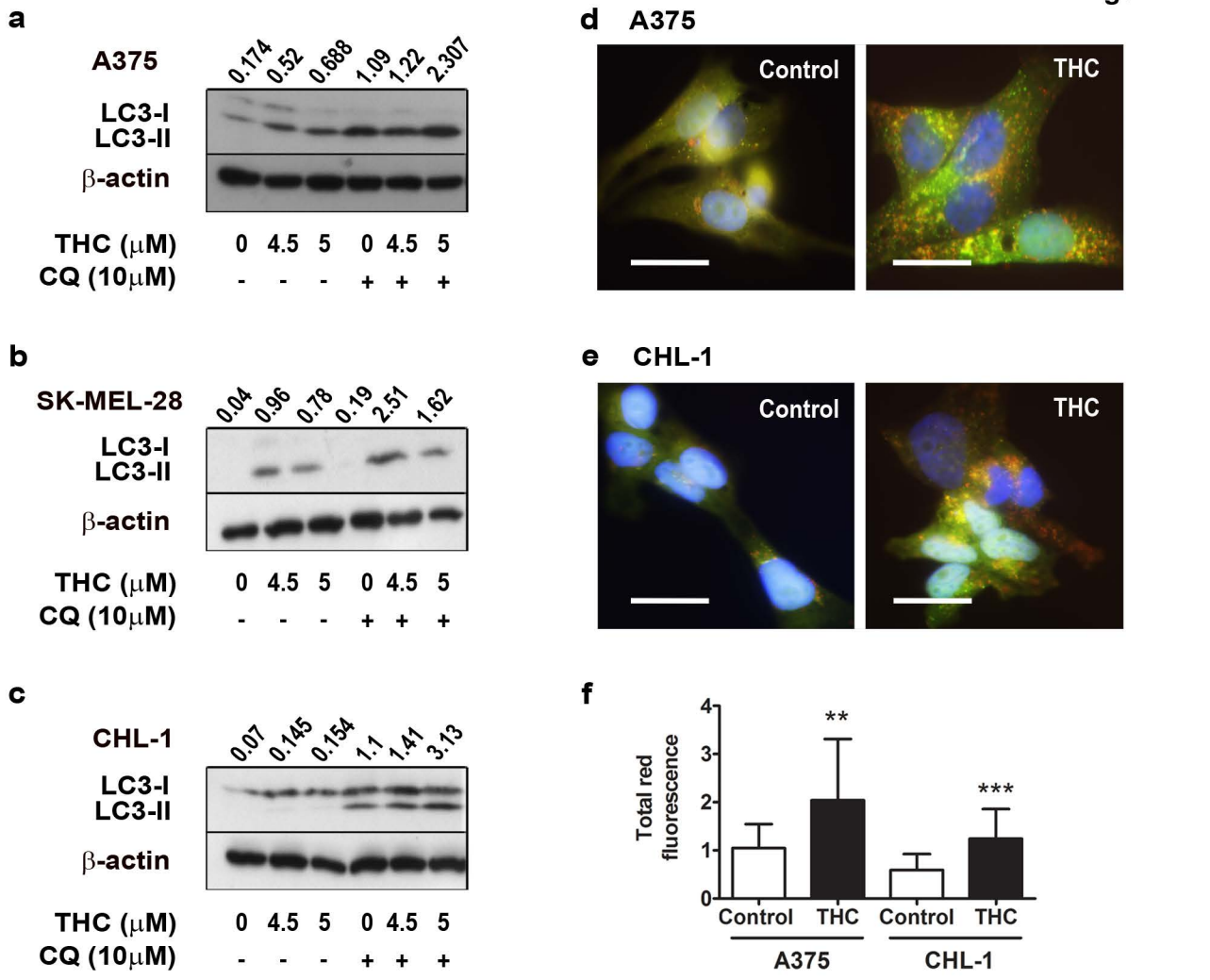
a
A375
0.174
0.52
0.688
1.09
1.22
2.307
LC3-I
LC3-II
β-actin
THC (μM) 0 4.5 5 0 4.5 5
CQ (10μM) - - - + + +
b
SK-MEL-28
0.04
0.96
0.78
0.19
2.51
1.62
LC3-I
LC3-II
β-actin
THC (μM) 0 4.5 5 0 4.5 5
CQ (10μM) - - - + + +
c
CHL-1
0.07
0.145
0.154
1.1
1.41
3.13
LC3-I
LC3-II
β-actin
THC (μM) 0 4.5 5 0 4.5 5
CQ (10μM) - - - + + +
d A375
Control
THC
e CHL-1
Control
THC
f
Total red fluorescence
4
3
2
1
0
**
***
Control
THC
Control
THC
A375
CHL-1

Figure 2

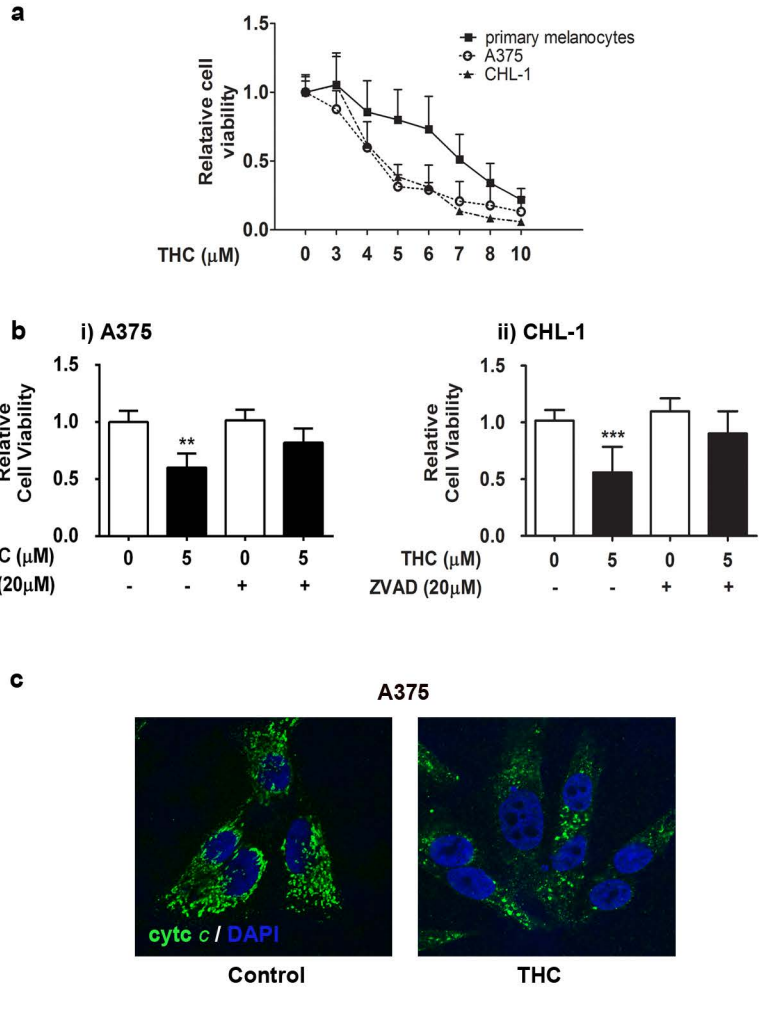
a
Relataive cell viability
1.5
1.0
0.5
0.0
primary melanocytes
A375
CHL-1
THC (μM)
0 3 4 5 6 7 8 10
b
i) A375
Relative Cell Viability
1.5
1.0
0.5
0.0
**
THC (μM)
0 5 0 5
ZVAD (20μM)
- - + +
ii) CHL-1
Relative Cell Viability
1.5
1.0
0.5
0.0
***
THC (μM)
0 5 0 5
ZVAD (20μM)
- - + +
c
A375
cytc c / DAPI
Control
THC

a

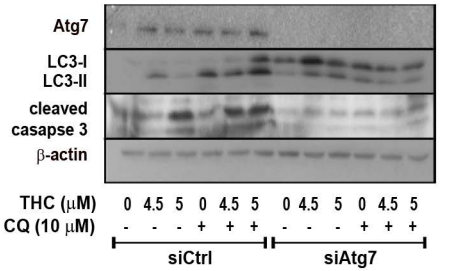
Atg7
LC3-I
LC3-II
cleaved
casapse 3
β-actin
THC (μM) 0 4.5 5 0 4.5 5 0 4.5 5 0 4.5 5
CQ (10 μM) - - - + + + - - - + + +
siCtrl
siAtg7

b

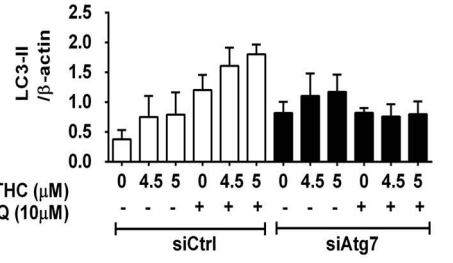
LC3-II
/β-actin
2.5
2.0
1.5
1.0
0.5
0.0
THC (μM) 0 4.5 5 0 4.5 5 0 4.5 5 0 4.5 5
CQ (10μM) - - - + + + - - - + + +
siCtrl
siAtg7

c

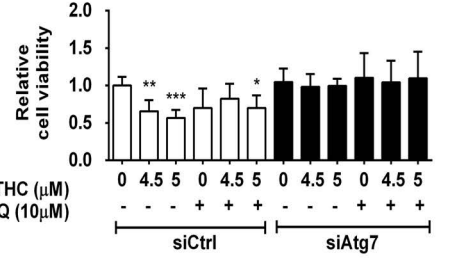
Relative
cell viability
2.0
1.5
1.0
0.5
0.0
**
***
*
THC (μM) 0 4.5 5 0 4.5 5 0 4.5 5 0 4.5 5
CQ (10μM) - - - + + + - - - + + +
siCtrl
siAtg7

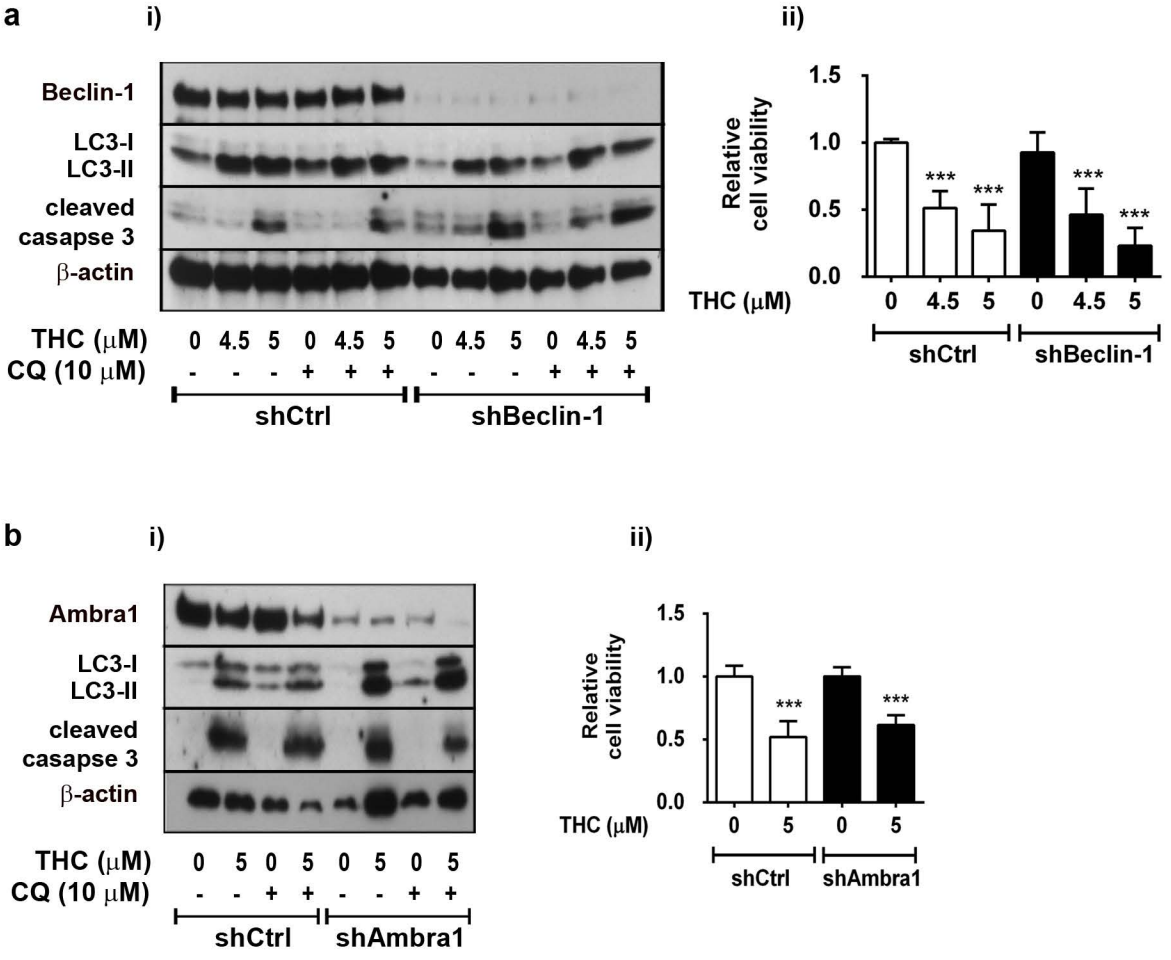
a
i)
Beclin-1
LC3-I
LC3-II
cleaved
casapse 3
β-actin
THC (μM) 0 4.5 5 0 4.5 5 0 4.5 5 0 4.5 5
CQ (10 μM) - - - + + + - - - + + +
shCtrl
shBeclin-1
ii)
Relative
cell viability
1.5
1.0
0.5
0.0
***
***
***
***
THC (μM) 0 4.5 5 0 4.5 5
shCtrl
shBeclin-1
b
i)
Ambra1
LC3-I
LC3-II
cleaved
casapse 3
β-actin
THC (μM) 0 5 0 5 0 5 0 5
CQ (10 μM) - - + + - - + +
shCtrl
shAmbra1
ii)
Relative
cell viability
1.5
1.0
0.5
0.0
***
***
THC (μM) 0 5 0 5
shCtrl
shAmbra1

a

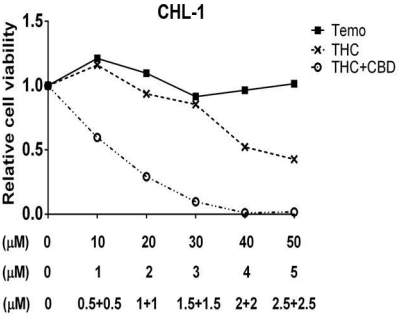
CHL-1
Relative cell viability
1.5
1.0
0.5
0.0
Temo
THC
THC+CBD
Temo (μM) 0 10 20 30 40 50
THC (μM) 0 1 2 3 4 5
THC+CBD (μM) 0 0.5+0.5 1+1 1.5+1.5 2+2 2.5+2.5

b

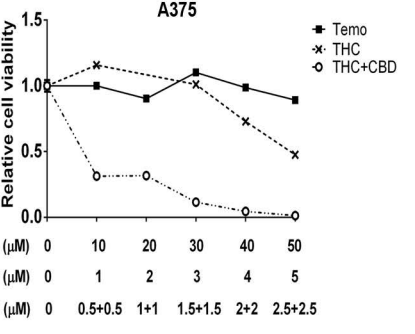
A375
Relative cell viability
1.5
1.0
0.5
0.0
Temo
THC
THC+CBD
Temo (μM) 0 10 20 30 40 50
THC (μM) 0 1 2 3 4 5
THC+CBD (μM) 0 0.5+0.5 1+1 1.5+1.5 2+2 2.5+2.5

b

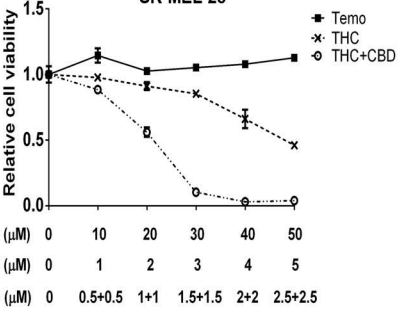
SK-MEL-28
Relative cell viability
1.5
1.0
0.5
0.0
Temo
THC
THC+CBD
Temo (μM) 0 10 20 30 40 50
THC (μM) 0 1 2 3 4 5
THC+CBD (μM) 0 0.5+0.5 1+1 1.5+1.5 2+2 2.5+2.5

Figure 6

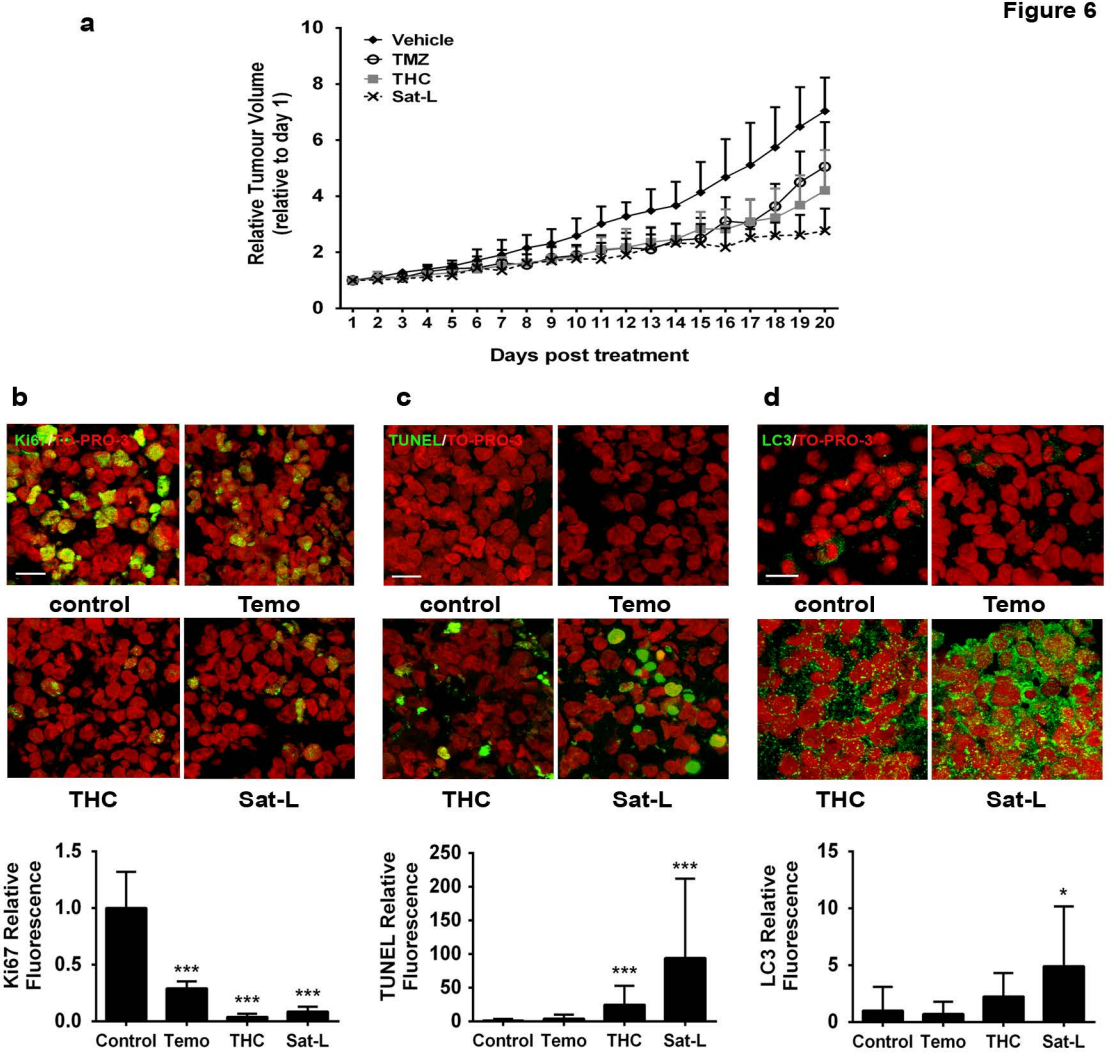
a
Vehicle
TMZ
THC
Sat-L
Relative Tumour Volume (relative to day 1)
Days post treatment
b
c
d
Ki67/TO-PRO-3
TUNEL/TO-PRO-3
LC3/TO-PRO-3
control
Temo
THC
Sat-L
Ki67 Relative Fluorescence
TUNEL Relative Fluorescence
LC3 Relative Fluorescence
Control
Temo
THC
Sat-L

Supplementary Figure 1

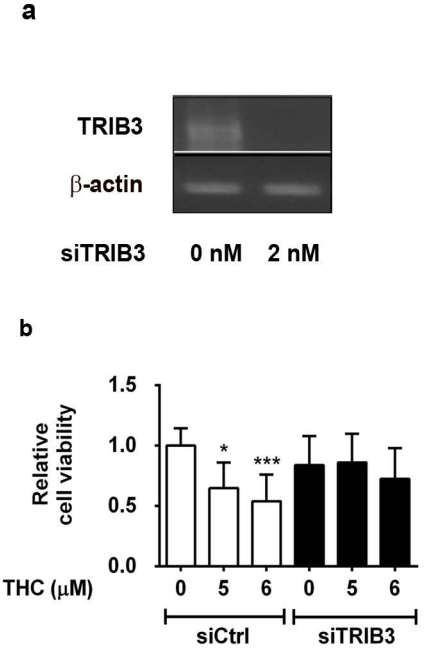

Supplementary Figure 2

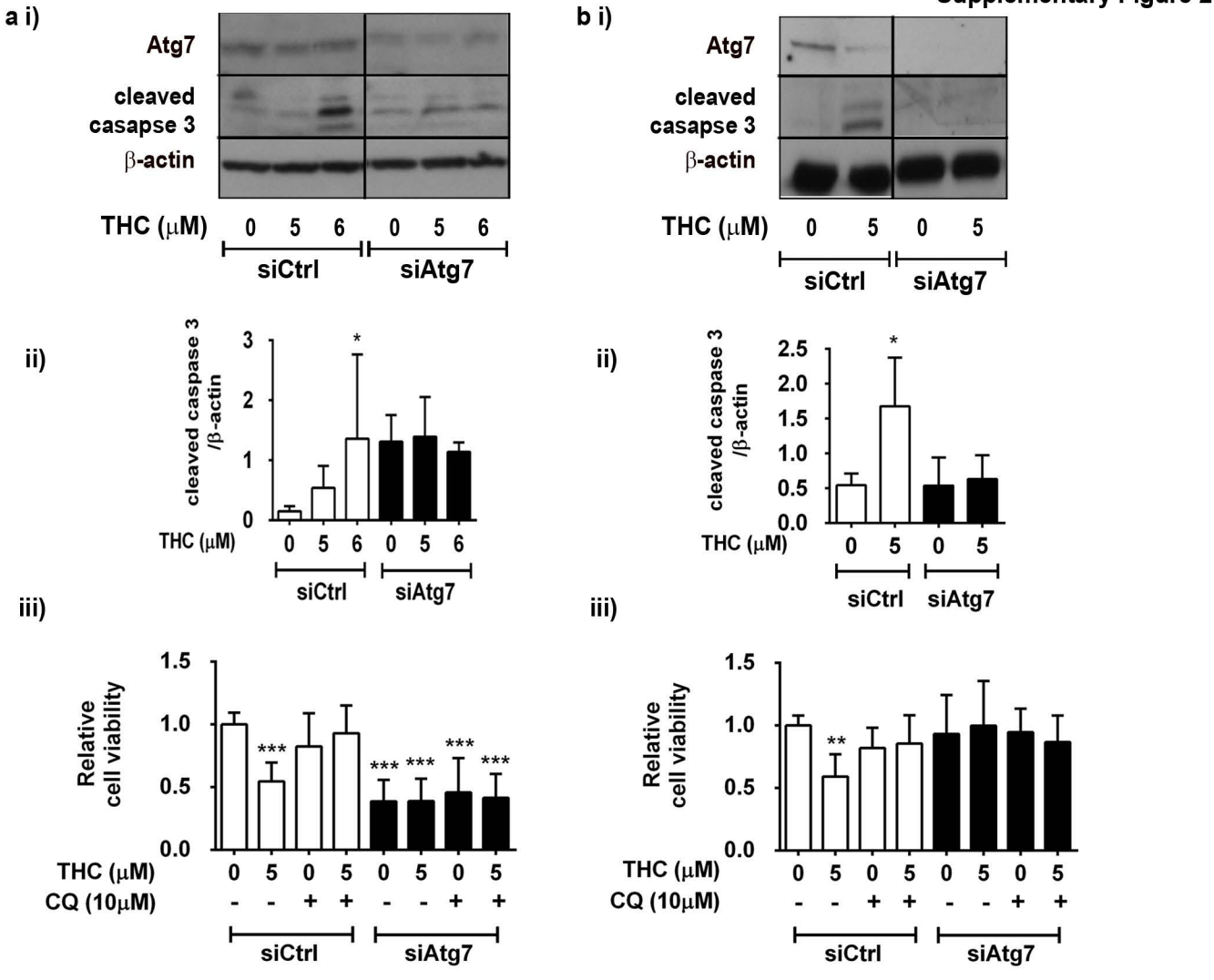

Supplementary Figure 3